The Single-Cycle Biphotons Generated by Noncollinear SPDC in The Chirped QPM Crystals

Jinbao Wang[1,2], and Haibo Lin[2]*

[1]College of Mechanical Engineering, Zhejiang University of Technology, Hangzhou 310014, China
[2] Institute of Mechanical & Electrical Technology, Taizhou Vocational & Technical College, Taizhou 318000, China
*Corresponding author: linhaibo_tzvtc@163.com

Abstract
We analysis the noncollinear spontaneous parametric down conversion(SPDC) and compare the biphotons generated by the chirped quasi-phase-matching(QPM) between the periodically poled lithium niobate(PPLN) and periodically poled $KTiOPO_4$(PPKTP) crystals. Due to the chirping of the crystals, the frequency response range of the biphotons would be greatly increased. For nonlinear SPDC, angular variation is limited (less than 0.06 degree in this paper), and the angle would narrow the frequency response range of the biphotons. We compare the effect of angle in PPLN crystals and PPKTP crystals for biphotons. Both the two crystals with chirped QPM, the single-cycle biphotons can be generated during noncollinear SPDC within a suitable angle range, which is favorable for wider applications in experiments.

Keywords*:* chirped QPM, biphotons, noncollinear, SPDC.

1.Introduction

An important theme in quantum optics is the generation of high quality broadband entangled states, such as the two or more photons with quantum correlations which are entangled each other. In recent decades, the entanglement has been considered as a basic tool for researching quantum information and shown wide application in several fields, including the quantum cryptography[1], quantum computation[2], quantum teleportation[3] and so on.

Nowadays, several techniques have been developed for the generation of the entangled photons with high quality broadband, and the most common and convenient one of which is that the entangled biphotons can be generated by the spontaneous parametric down-conversion(SPDC)[4][5][6][7]. In this process, the strongly pumped photon interacts with the nonlinear crystal and be split into two lower frequency ones named signal (with frequency ω_s) and idler (with frequency ω_i) photons, which are entangled with each other in multiple dimensions, e.g., frequency[8], polarization[9], and spatial shape[10][11]. Meanwhile, since the spectral bandwidth of the biphotons generated by SPDC is inversely proportional to the crystal length of the crystal, it provides a way to further broaden the spectral bandwidth[12][13]. However, the usefulness of this method is limited and other ways have been provided to broaden the spectral bandwidth, such as the designing of the optical parametric amplifiers(OPA)[14], the chirped quasi-phase-matching (QPM) crystal[15][16], or the chirped periodic poling structure for type I and type II[13][17][18][19], etc. Not only the pulse with wide bandwidth has been provided, but also the fundamental of temporal compression has been shown by these methods.

The amount of spatial entanglement of the biphotons generated by SPDC, which is deeply depending on the crystal length, the pump photons, and especially the used geometry (such as collinear or noncollinear SPDC)[7]. Lots of Refs.[7] [13][15][16][17][19][20][21][22][23] have pay attention on the collinear SPDC and found that chirp QPM crystals can broaden the frequency response range, generate the biphotons with high entanglement degree and ultrashort temporal width after the phase compensation. Some could even obtain the single-cycle lever, be viewed as ideal biphotons, with ultrashort temporal width (could be less than 5fs) and other favorable physical properties, such as high degree entanglement, and ultra-broadband, etc. In addition, the noncollinear SPDC in the PPLN crystals, which have been deeply discussed and probed in Ref.[24] , it is found that there is no significant distinction in the spectrum compared to the case of collinear when the angle θ is in the range of 0.25 ± 0.14 to -0.25 ± 0.14 degree, and the temporal width of the sum frequency generation (SFG) can still reaches 4.4 fs (about 1.2 cycle) in the noncollinear case.

There are many crystals that enable parametric down conversion, such as β −barium borate (BBO)[25][26], lithium niobate (LN), and potassium titanyl phosphate ($KTiOPO_4$ or KTP for short), etc. Of these, when the crystals are quasi-phase-matched structures, the PPLN and PPKTP crystals are the most widely studied[27]. In particular, PPLN crystals, due to their unique crystal structure, have been widely used both theoretically and experimentally[28], including for noncollinear SPDC[29].

This paper is mainly in comparing the characteristics of the spectral distribution of the biphotons generated by the chirped QPM PPLN and PPKTP crystals, in the noncollinear SPDC, as well as the temporal widths of the entangled biphotons with the help of the phase compensated effect. In order to facilitate the comparison, we select pump lights with different frequencies incident into the two nonlinear crystals according to their refractive indices so that they can generate the ultra-broadband biphotons. Meanwhile, considering that too large a noncollinear angle can distort the SPDC process, we set the noncollinear angle within the range of ±0.06 degrees. In this angular range, a broadband biphotons spectrum can be obtained, and then the spectral distribution can be converted

This provisional PDF is the accepted version. The article should be cited as: J. Eur. Opt. Society-Rapid Publ., https://doi.org/10.1051/jeos/2024004

from the frequency domain to the temporal domain with the help of the Fourier transformation. According to the method shown in Ref.[16], the temporal domain pulse can be compressed after perfect phase compensation, and the temporal width of the pulse can be measured by homodyne detection. The single cycle ultrashort biphotons pulse can be generated in the two nonlinear crystals.

2. The Noncollinear SPDC in Chirped QPM Crystal

In the noncollinear SPDC, three significant factors would be considered: the pump photon, the nonlinear crystal and the phase mismatching function among the three mixed waves.

Firstly, it is assumed that the pump, signal and idler photons are extraordinary light, and they can be expressed by the creation and annihilation operators as follows[30]:

$$E_{\mu\hat{e}}(r,t) = \frac{i}{2\pi}\int\left[|n_e(k)|^{-1}(h\upsilon_e)^{1/3}a_{e\mu}(k)e^{ikr-i\omega t}\hat{e}(k)+|n_e(k)|^{-1}(h\upsilon_e)^{1/3}a^{\dagger}_{e\mu}(k)e^{ikr+i\omega t}\hat{e}(k)\right]dk \quad (1)$$

where $\mu = p, s, i$ represents the pump, signal and idler photons, respectively. $a_e^{\dagger}$ and a_e are the creation and annihilation operators for extraordinary photons with poling vectors $\hat{e}(k)$. According to the method shown in Ref.[16], the pump photon is viewed as a monochromatic one, and assume that the ones incident into the PPLN and PPKTP crystal with the central frequencies written as ω_{p_1} and ω_{p_2}, respectively. The corresponding central wave lengths are set as $\lambda_{p_1} = 0.42\mu m$ and $\lambda_{p_2} = 0.523\mu m$. For simplicity, the monochromatic pump is independent with time, and expressed as: $E_{p_{1,2}} = \int E_{p_0}\delta(\omega - \omega_{p_{1,2}})d\omega$.

Secondly, for the expression of the nonlinear crystal. When the pump photon incidents into the crystal and interact with it, the down-conversion efficiency would reduce as the light propagating along it, which is called the Poynting walk-off effect. To solve this problem, J. Armstrong[31] proposed a way by designing periodically poled grating with alternate reversal poled directions which is called as quasi-phase-matching (QPM). These poled gratings in QPM, which can steadily increase the efficiency of down-conversion, expressed by Fourier expansion forms shown as following[32]:

$$\mathrm{d}(z) = d_{eff}\sum_{m=-\infty}^{\infty} G_m * exp(-ik_m z) \quad (2)$$

where d_{eff} is the effective nonlinear coefficient of the nonlinear crystal, and $k_m = 2\pi m/\Lambda$ is the mth grating vector with Fourier form. Λ is the poled grating period, which can be viewed as constant for the general QPM. However, the poled grating periods associated with position z can be written as $\Lambda(z)$ for the chirped QPM. In this paper, we consider the crystals with linear chirp rate, and the spatial wave vector $\mathrm{K}(z)$ is as the function of position z which determines the grating periods, can be expressed as:

$$\mathrm{K}(z) = \frac{2\pi}{\Lambda(z)} = \frac{2\pi}{\Lambda_0} - \zeta z = K_0 - \zeta z \quad (3)$$

Where K_0 is the spatial wave vector at the incident end of the nonlinear crystal that can be perfectly phase-matched with respect to the first poled grating period Λ_0. $\Lambda(z)$ is the poled grating period function with the position z. And the spatial phase can be accumulated by the chirp rate ζ and formed as follows:

$$\phi(z) = \int_0^z \zeta z dz = \frac{\zeta^2}{2} \quad (4)$$

The spatial phase with chirp rate, plays a significant role for the coupling equation for the three mixed waves which can be shown as follows[16][32]:

$$\frac{dE_s}{dz} = i\chi E_i^* e^{i[\Delta kz+\phi(z)]} \quad (5)$$

$$\frac{dE_i^*}{dz} = -\chi^* E_s e^{-i[\Delta kz+\phi(z)]} \quad (6)$$

Where χ is a parameter associated with the factors such as the pump spectral amplitude, the nonlinear crystal refractive index, nonlinear effective coefficient and the interaction with the pump and the crystal. It can be viewed as constant for it slowly varies with the position. The decisive roles are played by the frequency relationship and the phase matching function which show the energy and angular momentum conservations for the three mixed waves coupling equations, respectively. They can be expressed as:

$$\omega_p = \omega_s + \omega_i \quad (7)$$

$$\Delta\mathrm{k}(\omega_s, \omega_i, z) = k_p(\omega_p) - k_s(\omega_s) - k_i(\omega_i) - K(z) \quad (8)$$

Here $k_\mu = n_e(\omega_\mu)\omega_\mu/c$ denotes the wave vectors of pump, signal and idler photons and e represents the extraordinary lights. Equation (7) can be applied with the condition of pump photon is monochromatic, Hence, for simplicity, we denote the signal frequency as ω, and the idler frequency as $\omega_p - \omega$.

Figure 1. *Scheme of noncollinear SPDC in a chirped QPM crystal. The directions of arrows represent polarized axis for the QPM PPLN or PPKTP crystals. p, s, i represent the pump, signal and idler lights.*

For the noncollinear SPDC, the monochromatic pump propagating in the crystal and split into two lower frequency photons with the angle θ relative to the pump propagation direction as shown in Figure 1. The process satisfies the energy and angular momentum conservations. And the phase mismatching function shown in equation (8) plays a significant role during SPDC, which determines the parameter gain and the conversion efficiency[14]. In noncollinear SPDC, the signal and idler photons propagate through the nonlinear crystal with the angle θ relative to the pump propagation direction. Hence, the phase mismatching function Δk in equation (8) can be rewritten as the function of angle θ according to the Ref.[24]:

$$\Delta k(\omega,\theta,z) = k_p(\omega_p) - k_s(\omega)\sqrt{1-\left[\frac{\sin\theta}{n_e(\omega)}\right]^2} - k_i(\omega_p-\omega)\sqrt{1-\left(\frac{\omega}{\omega_p-\omega}\right)^2\left[\frac{\sin\theta}{n_e(\omega_p-\omega)}\right]^2} - K(z) \quad (9)$$

In Ref.[24], the angle θ in noncollinear SPDC has been demonstrated in theory and verified in experiment in the range of $\pm 0.25 \pm 0.14$ degree.

In collinear SPDC, $\theta = 0$, the generated biphotons in the same mode can be separated with the help of dichroic filter in the propagation path. And in noncollinear case, $\theta \neq 0$, the two photons can propagate along their own path, without the help of dichroic filter, which makes its application more convenient[24].

The joint spectral amplitude function(JSAF) for the noncollinear SPDC can be calculated by solving the coupling equations (5) and (6) and shown as following[15][23]:

$$T(\omega,\theta) \propto exp\left[-\frac{i\Delta k^2(\omega,\theta)}{2\zeta}\right]\left\{erfi\left[\frac{(1+i)\Delta k(\omega,\theta)}{2\sqrt{\zeta}}\right] + erfi\left[\frac{(1+i)(\Delta k(\omega,\theta)+\zeta L)}{2\sqrt{\zeta}}\right]\right\} \quad (10)$$

where erfi is the imaginary error function. And JSAF $T(\omega,\theta)$ is a function associated with the frequency ω and angle θ and represents the interaction between the three mixed waves and the nonlinear crystal. The squared modulus of JSAF $|T(\omega,\theta)|^2$ is the spectral function which indicates the probability of the detecting biphotons. And nearly other spectral temporal properties are determined by the JSAF.

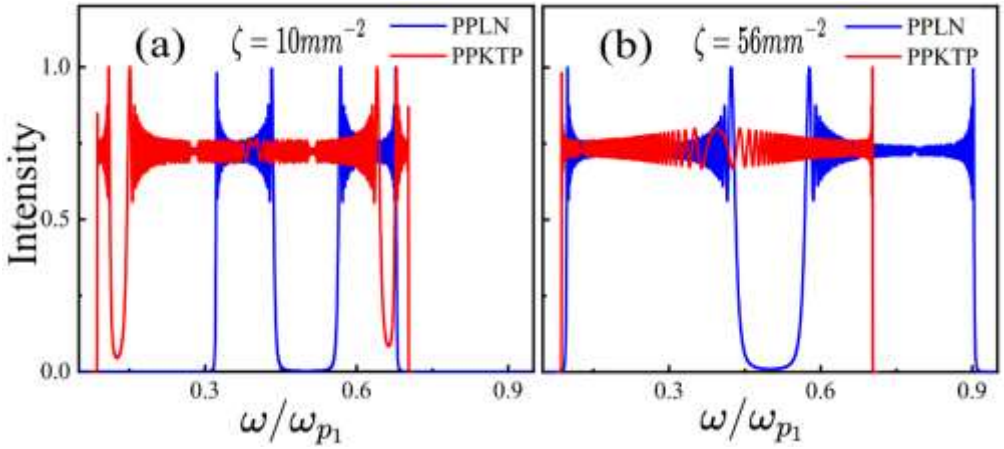

Figure 2. *The spectral intensity of the biphotons generated by noncollinear SPDC in the PPLN (blue line) crystal and PPKTP (red line) crystal with* $\theta = 0.01$ *degree and the chirp rate: (a).*$\zeta = 10mm^{-2}$*; (b).* $\zeta = 56mm^{-2}$.

3. Results and Discussions

The frequency relationship between the signal and idler photons satisfy equation (7) when the pump is monochromatic. The intensity distribution of JSAF $T(\omega, \theta = 0.01)$ versus frequency with $\theta = 0.01$ degree is shown in Figure 2. In this figure, the intensity distribution of JSAF in PPLN crystals (blue lines) are consistent with the results of Ref.[22], which means that the main influence of JSAF is the chirp rate rather than the angle when the angle is small. As the chirp rate increases, the width of the spectral frequency response becomes progressively broader, a law that also applies to the case of PPKTP crystals (red line in the figure). In addition, the comparison in Figure 2 shows that the frequency response range of the PPKTP crystal is larger when the chirp rate is smaller. As the chirp rate increases, the frequency response range of the PPLN crystal becomes wider and exceeds that of the PPKTP crystal. Meanwhile, the intensity distribution of JSAF in the PPLN crystal is two rectangular-like shape symmetric about $0.5\omega_{p_1}$. The intensity distribution of JSAF which symmetric about $0.5\omega_{p_2}$ in PPKTP crystals is originally composed of three rectangle-like shapes when the chirp rate $\zeta = 10mm^{-2}$. As the chirp rate increase, the two concave parts on the two sides gradually disappear and form an overall symmetric rectangle-like shapes. The increased frequency response range in this case is mainly caused by the disappearance of these two concave parts.

In order to further clearly describe the physical characteristics of JSAF, we assume that the signal and idler photons are independent of each other. Figure 3 and Figure 4 show the interaction between the pump photon and the chirped QPM crystals, PPLN and PPKTP, respectively. The left columns of the two figures show the spectral density distribution with $\theta = 0.06$ degree, which are not significant different from the case with $\theta = 0.01$ degree. A detailed comparison has been conducted by making $\Delta T = |T(\omega_s, \omega_i, \theta = 0.06) - T(\omega_s, \omega_i, \theta = 0.01)|$, and the difference distribution of ΔT has been shown in the right columns of Figure 3 and Figure 4. It can be found that most areas of ΔT tend towards zero, which also means that there is not much difference in JSAF between $\theta = 0.01$ and 0.06 degrees. The most obvious areas are at the edges of each JSAF. The bright color at the edge indicates a large value of ΔT, due to the fact that when $\theta = 0.01$ degree, a small portion of the spectral response range is added at the edge, making the difference at the edge the most significant. In addition, bright ripples also appeared in the middle region of ΔT, mainly due to the chirping of the poled grating periods in nonlinear crystals. The higher the chirp rate, the wider the frequency response range, and the more obvious the bright ripple. Meanwhile, comparing PPLN and PPKTP crystals, it can be found that with the same chirp rate, the bright ripples of PPKTP crystals are more abundant. The main reason for this is that the value of Δk in Figure 5 tends toward zero.

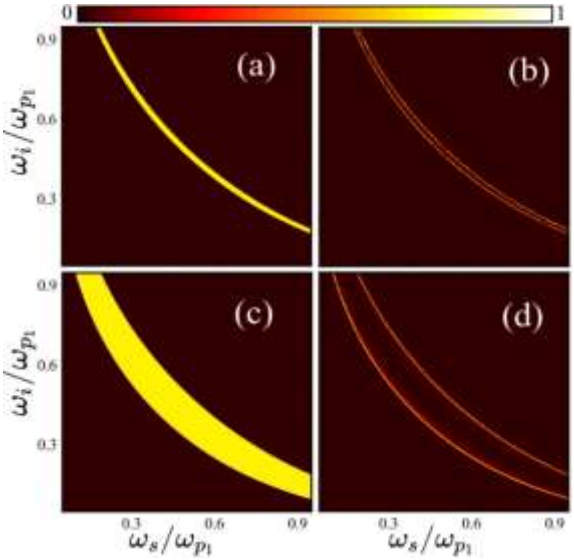

Figure 3. *The spectral power distribution for JSAF in PPLN crystal with chirp rate $\zeta = 10mm^{-2}$ in (a) & (b) and $\zeta = 56mm^{-2}$ in (c) & (d). Here, the left column plot (a) and (c) with $\theta = 0.06$ degree and the right column plot (b) and (d) represent $\Delta T = |T(\theta = 0.06) - T(\theta = 0.01)|$.*

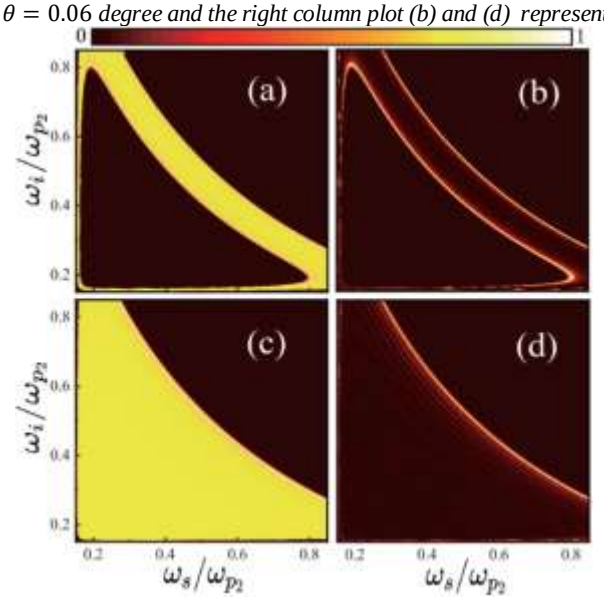

Figure 4. *The spectral power distribution for JSAF in PPKTP crystal with chirp rate $\zeta = 10mm^{-2}$ in (a) & (b) and $\zeta = 56mm^{-2}$ in (c) & (d). Here, the left column plot (a) and (c) with $\theta = 0.06$ degree and the right column plot (b) and (d) represent $\Delta T = |T(\theta = 0.06) - T(\theta = 0.01)|$.*

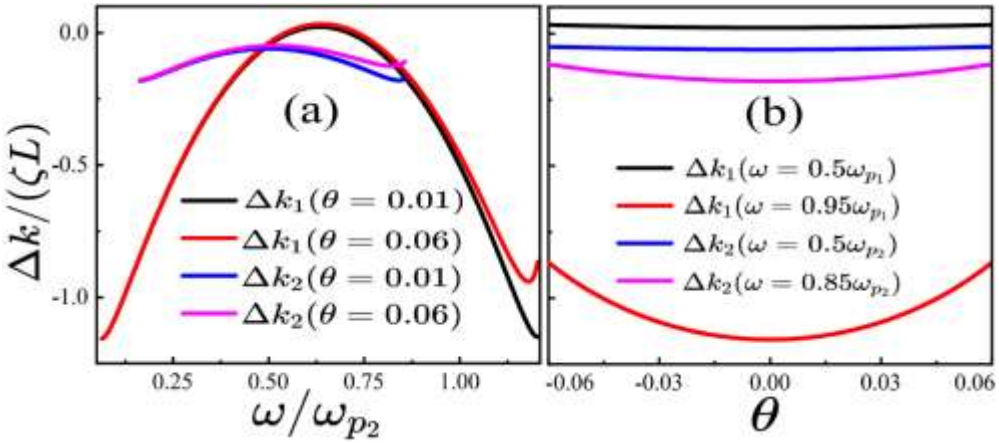

Figure 5. *(a).Phase mismatching function Δk per ζL versus frequency ω/ω_p with different angles; (b). Phase mismatching function Δk versus angle θ with different frequencies. Subscripts 1 and 2 represent PPLN and PPKTP crystals, respectively.*

From Figure 5(a), it can be found that, in generally, the Δk frequency response range of PPLN crystals is larger than that of PPKTP crystals, which is consistent with the conclusions in Figure 3 and Figure 4. Although the frequency response range of PPKTP crystal is small, its phase mismatching function Δk is closer to zero. It means that this situation has a better phase matching effect if without considering phase compensation. In addition, when $\theta = 0.01$ degree becomes 0.06 degree, Δk basically remains in its original state. But the main difference is that when ω is large, the right side of the Δk in Figure 5(a) is slightly raised, and the symmetry of the original image is also disrupted. This is consistent with the physical picture of noncollinear SPDC, as well as the conclusions obtained in Figure 3 and Figure 4. As shown in Figure 5(b), it can be found that both in PPLN and PPKTP crystals, when ω is small, the varying of θ in the range $-0.06 \rightarrow 0.06$ cannot cause obvious changes in Δk. However, when ω is large, the varying of θ in this range would lead to the changes in Δk, which is consistent with the conclusion in Figure 5(a).

Based on the above discussion, chirped QPM crystals broaden the spectral range of the generated biphotons pulses, the frequency domain can be converted to the temporal domain through Fourier transform limited. According to the method shown in Ref.[16], the quadratic mismatching phase can be compensated by the function as shown in following:

$$\mathrm{CF}(\omega,\theta) = exp\left[i\left(\frac{\Delta k(\omega,\theta)^2}{2\zeta}\right) - i\big(k_s(\omega) + k_i(\omega)\big)L\right] \tag{11}$$

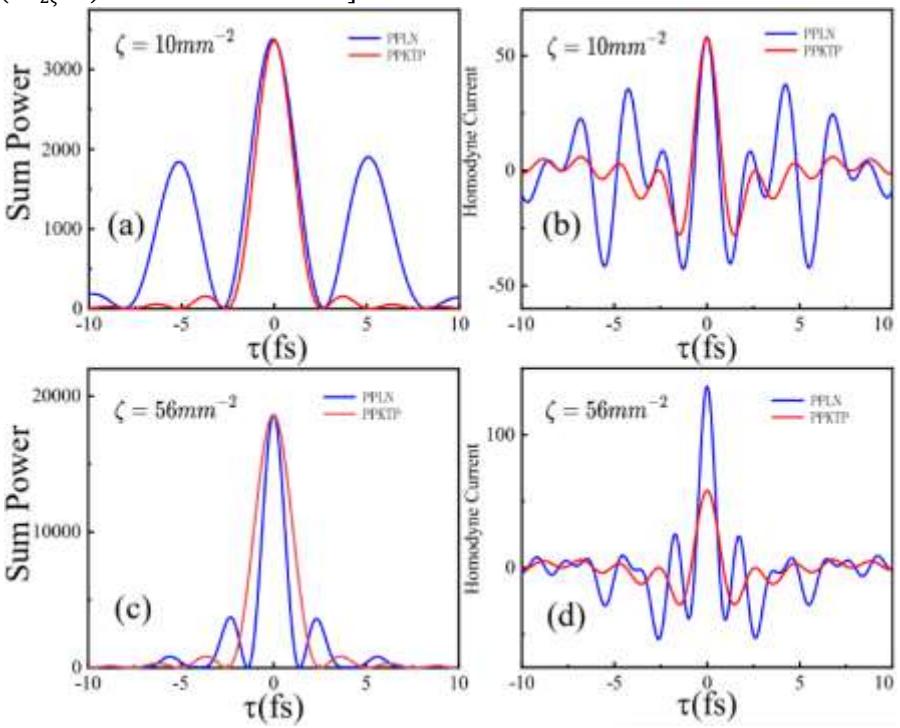

Figure 6. *Normalized sum power with (a). $\zeta = 10mm^{-2}$ and (c). $\zeta = 56mm^{-2}$. The homodyne current detected by homodyning detection with (a). $\zeta = 10mm^{-2}$ and (c). $\zeta = 56mm^{-2}$. The angle for the noncollinear SPDC is $\theta = 0.06$ degree.*

As discussion above, the signal and idler photons generated by collinear SPDC can be separated through filters. However, for noncollinear, the signal and idler photons can be automatically separated through their respective propagation paths. With the help of the perfect phase compensation function in equation (11), the signal and idler photons can arrival at the correlator and generate sum frequency pulses. This pulse has the same central frequency with the original pump light. Therefore, their sum power and homodyne current can be detected by homodyning detection, the temporal width and their cycle number can also be further calculated.

As shown in Figure 6(a) and (b), it can been found that when $\theta = 0.06$ degree, $\zeta = 10mm^{-2}$, the temporal widths of biphotons are 2.67fs and 2.30 fs, with 1.9 and 1.29 cycles generated in the PPLN and PPKTP, respectively. Hence, the biphotons generated in PPKTP crystal shows shorter temporal width in this case. The reason is that the response frequency range in PPKTP would be wider than in PPLN with $\zeta = 10mm^{-2}$, as shown in Figure 2(a). However, when $\zeta = 56mm^{-2}$ in Figure 6(c) and (d), the temporal widths of biphotons are 1.3 fs and 2.24 fs, with 0.93 and 1.26 cycles generated in the PPLN and PPKTP, respectively. The biphotons generated in PPLN crystal shows shorter temporal width in this case. The reason is that the response frequency range in PPLN would be wider than in PPKTP with $\zeta = 56mm^{-2}$, as shown in Figure 2(b). Hence, both the two chirped QPM crystal can generate the single cycle biphotons in noncollinear SPDC.

4.Conclusion

We analysis the noncollinear SPDC and compare the biphotons generated by the chirped QPM between the PPLN and PPKTP crystals. The chirp of the crystal makes the biphotons' spectral bandwidth be wider, and the temporal width be shorter. Angular variation is limited to be less than 0.06 degree in this paper. In this angular range, the angle plays main significant role on the boundary of response frequency range, the larger angle would make the response frequency range be narrower. The single cycles biphotons with different spectrum bands and temporal widths can be generated in the two crystal with different chirp rates in a

noncollinear SPDC. We hope that our work can help to simplify the experimental generation of ultrashort pulses of entangled biphotons in further.

Acknowledgement

This work was supported by General scientific research project of Zhejiang Provincial Department of Education (Grant No. Y202250327), Taizhou Science and Technology Project (Grant No. 22gyb17), and Taizhou High-level Talent Special Support Program (2019, 2020). Skills Master Studio in Taizhou City of Zhejiang Province (Tai Talent Link [2022] No. 48). J.W sincerely thanks S. E. Harris for his Mathematica codes.

Authors' contributions

JW proposed the original idea, gave advices and wrote the manuscript. HL implemented the work. The progress is a result of common contributions and discussions of JW and HL. Both authors read and approved the final manuscript.

Competing interests

The authors declare that they have no competing interests.

Reference

[1]. K. Ekert, Quantum cryptography based on Bell's theorem，Phys. Rev. Lett. 67, 661(1991)

[2]. M. A. Nielsen and I. L. Chuang, Quantum Computation and Quantum Information (Cambridge University Press, 2000)

[3]. C. H. Bennett, G. Brassard, C. Crepeau, R. Jozsa, A. Peres, and W. K. Wootters, Teleporting an unknown quantum state via dual classical and Einstein-Podolsky-Rosen channels, Phys. Rev. Lett. 70, 1895(1993).

[4]. C. K. Hong, Z. Y. Ou, and L. Mandel, Measurement of subpicosecond time intervals between two photons by interference, Phys. Rev. Lett. 59, 2044 (1987).

[5]. P. G. Kwiat, K. Mattle, H. Weinfurter, A. Zeilinger, A. V. Sergienko, and Y. H. Shih, New High-intensity source of polarization-entangled photon pairs, Phys. Rev. Lett. 75, 4337 (1995).

[6]. J. P. Torres, K. Banaszek, and I. A. Walmsley, Chapter 5 - Engineering Nonlinear Optic Sources of Photonic Entanglement, Prog. Opt. 56, 227 (2011).

[7]. J. Svozil´ık, J. Pe˘rina and J. P. Torres, High spatial entanglement via chirped quasi-phase-matched optical parametric down-conversion, Phys. Rev. A 86,052318(2012)

[8]. C. K. Law, I. A. Walmsley, and J. H. Eberly, Continuous Frequency Entanglement: Effective Finite Hilbert Space and Entropy Control, Phys. Rev. Lett. 84, 5304 (2000).

[9]. P. G. Kwiat, K. Mattle, H. Weinfurter, A. Zeilinger, A. V. Sergienko, and Y. Shih, New High-Intensity Source of Polarization-Entangled Photon Pairs, Phys. Rev. Lett. 75, 4337 (1995).

[10]. H. H. Arnaut and G. A. Barbosa, Orbital and Intrinsic Angular Momentum of Single Photons and Entangled Pairs of Photons Generated by Parametric Down-Conversion, Phys. Rev. Lett. 85, 286 (2000).

[11]. A. Mair, A. Vaziri, G. Weihs, and A. Zeilinger, Entanglement of the orbital angular momentum states of photons, Nature (London)412, 313 (2001).

[12]. E. Dauler, G. Jaeger, A. Muller, A. L. Migdall, and A. V. Sergienko, Tests of a Two-Photon Technique for Measuring Polarization Mode Dispersion With Subfemtosecond Precision, J. Res. Natl. Inst. Stand. Technol. 104, 1 (1999)

[13]. A. Fraine, O. Minaeva, D. S. Simon, R. Egorov and V. Sergienko, Broadband source of polarization entangled photons, Opt. Lett. 37,11,1910,(2012)

[14]. M. Charbonneau-Lefort, B. Afeyan, and M. M. Fejer, Optical parametric amplifiers using chirped quasi-phase-matching gratings I: practical design formulas, J. Opt.Soc. Am. B 25, 463 (2008)

[15]. M. A. Arbore, O. Marco, and M. M. Fejer, Pulse compression during second-harmonic generation in aperiodic quasi-phase-matching gratings, Opt. Lett. 22, 865(1997)

[16]. Harris, Chirp and Compress: Toward Single-Cycle Biphotons, Phys. Rev.Lett. 98, 063602,(2007)

[17]. S. Carrasco, J. P. Torres, L. Torner, A. V. Sergienko, B. Saleh, and M. C. Teich, Enhancing the axial resolution of quantum optical coherence tomography by chirped quasi-phase matching, Opt. Lett. 29, 2429 (2004).

[18]. S. Carrasco, M. Nasr, A. V. Sergienko, B. Saleh, M. C. Teich, J. P. Torres, and L. Torner, Broadband light generation by noncollinear parametric downconversion, Opt. Lett. 31, 253 (2006).

[19]. M. Nasr, S. Carrasco, B. Saleh, A. V. Sergienko, M. C. Teich, J. P. Torres, L. Torner, D. Hum, and M. Fejer, Ultrabroadband Biphotons Generated via Chirped Quasi-Phase-Matched Optical Parametric Down-Conversion, Phys. Rev. Lett. 100, 183601 (2008).

[20]. G. Brida, M. V. Chekhova, I. P. Degiovanni, M. Genovese, G. Kh. Kitaeva, A. Meda and O. A. Shumilkina, Chirped Biphotons and their Compression in Optical Fibers, Phys. Rev.Lett.103,193602(2009)

[21]. J. S. Zhao, L. Sun, X. Q. Yu, J. F. Wang, H. Y. Leng, Z. D. Xie, Y. L. Yin, P. Xu and S. N. Zhu, Broadband continuous-variable entanglement source using a chirped poling nonlinear crystal, Phys. Rev. A. 81.013832(2010)

[22]. D. B. Horoshko and M. I. Kolobov, Towards single-cycle squeezing in chirped quasi-phase-matched optical parametric down-conversion, Phys. Rev. A.88.033806(2013)

[23]. D. B. Horoshko and M. I. Kolobov, Generation of monocycle squeezed light in chirped quasi-phase-matched nonlinear crystals, Phys. Rev. A.95.033837(2017)

[24]. Akira Tanaka *et al*, Noncollinear parametric fluorescence by chirped quasi-phase matching for monocycle temporal entanglement, Opt. Express, 20,25228 (2012)

[25]. Y. Zhao, S. Zhang, Z. Zhang, Z. Dong, D. Chen, Z. Zhang, and Y. Xia, Influence of geometrical configuration on molecular vibrational dynamics in BBO crystals studied by femtosecond CARS, Optics & Laser Technology,64, 120 (2014)
[26]. J. Saha, S. Deb, Fourth harmonic generation of Laguerre Gaussian beam in BBO crystal by total internal reflection-quasi phase matching technique, Optik, 254, 168689, (2022)
[27]. S. Guo, K. Shang, High-flux, high-visibility entangled photon source obtained with a non-collinear type-II PPKTP crystal pumped by a broadband continuous-wave diode laser, Opt. Comm., 545, 129586, (2023)
[28]. J. Liñares, G. M. Carral, X. Prieto-Blanco and D. Balado, Autocompensating measurement-device-independent quantum cryptography in space division multiplexing optical fibers, J. Eur. Opt. Soc.-Rapid Publ. 17, 19(2021)
[29]. L. Moscardi, S. Varas, A. Chiasera, F. Scotognella and M. Guizzardi, Ultrafast broadband optical modulation in indium tin oxide/titanium dioxide 1D photonic crystal,J. Eur. Opt. Society-Rapid Publ. 18, 8 (2022)
[30]. C.L.Tang and L.K.Cheng, Fundamentals of optical parametric processes and oscillators, Harwood academic publishers.
[31]. J. A. Armstrong, N. Bloembergen, J. Ducuing, and P. S. Pershan, Interactions between Light Waves in a Nonlinear Dielectric, Phys. Rev.127, 1918 (1962).
[32]. L. E. Myers, R. C. Eckardt, M. M. Fejer, R. L. Byer, W. R. Bosenberg and J. W. Pierce, Quasi-phase-matched optical parametric oscillators in bulk periodically poled LiNbO3, J. Opt. Soc. Am. B, 12, 2102 (1995).